IL NUOVO CIMENTO Vol. 36 C, N. 1 Gennaio-Febbraio 2013
DOI 10.1393/ncc/i2013-11429-2

Colloquia: IFAE 2012

Search for the Standard Model Higgs boson in the $WW^{(\star)}$ decay mode with ATLAS

M. Biglietti
INFN, Sezione di Roma Tre - Roma, Italy

ricevuto il 31 Agosto 2012

Summary. — A search for the Standard Model Higgs boson in the $H \to WW^{(\star)} \to \ell\nu\ell\nu$ ($\ell = e, \mu$) decay modes is presented. The search is performed using proton-proton collision data corresponding to an integrated luminosity of $4.7\,\text{fb}^{-1}$ at a centre-of-mass energy of 7 TeV collected during 2011 with the ATLAS detector at the Large Hadron Collider. No significant excess of events over the expected background is observed. An upper bound is placed on the Higgs boson production cross section as a function of its mass. A Standard Model Higgs boson with mass in the range between 133 GeV and 261 GeV is excluded at 95% confidence level, while the expected exclusion range is from 127 GeV to 233 GeV.

PACS 13.75.Cs – Nucleon-nucleon interactions (including antinucleons, deuterons, etc.).
PACS 13.85.-t – Hadron-induced high- and super-high-energy interactions (energy > 10 GeV).
PACS 14.80.Ec – Other neutral Higgs bosons.
PACS 14.80.Bn – Standard-model Higgs bosons.

1. – Introduction

A primary goal of the Large Hadron Collider (LHC) is to test the Standard Model mechanism of electroweak symmetry breaking by searching for Higgs boson production in high-energy proton-proton collisions. The Higgs boson is the only elementary particle in the Standard Model (SM) of particle physics that has not yet been observed. It is intimately related to the Higgs mechanism [1, 2], which in the SM gives mass to all other massive elementary particles. The analysis described in this paper uses the full 2011 dataset, which after requiring that all detector components are fully functional corresponds to $4.7\,\text{fb}^{-1}$ of proton-proton (pp) collisions at $\sqrt{s} = 7\,\text{TeV}$. Details are available in [3].

2. – Event selection and background estimation

The data were collected using inclusive single-muon and single-electron triggers.

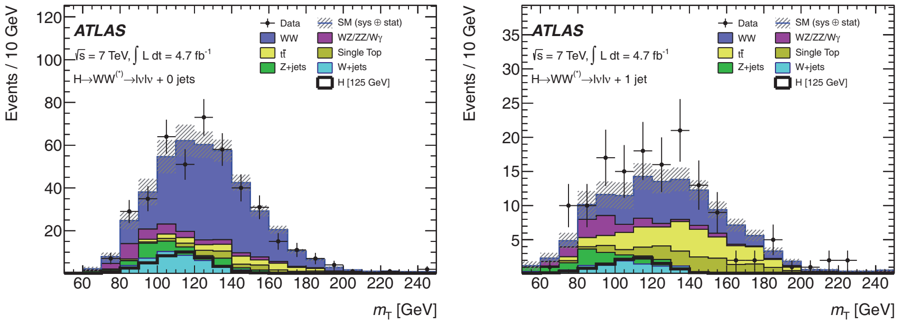

Fig. 1. – Transverse mass, m_{T}, distribution in the 0-jet (right) and 1-jet (left) channels, for events satisfying all criteria for the low m_H selection. The lepton flavours are combined. The expected signal for a SM Higgs boson with $m_H = 125\,\mathrm{GeV}$ is superimposed. The hashed area indicates the total uncertainty on the background prediction.

$H \to WW^{(\star)} \to \ell\nu\ell\nu$ candidates (with $\ell = e, \mu$) are pre-selected by requiring exactly two oppositely charged leptons with p_{T} thresholds of 25 GeV and 15 GeV for the leading and sub-leading lepton, respectively. For muons (electrons), the range $|\eta| < 2.4$ ($|\eta| < 2.47$) is used. Leptons from heavy-flavour decays and jets satisfying the lepton identification criteria are suppressed by requiring the leptons to be isolated. Drell-Yan background and multijet production via QCD processes are suppressed by requiring the dilepton invariant mass to differ from the Z-boson mass and large $E_{\mathrm{T}}^{\mathrm{miss}}$. After the isolation and $E_{\mathrm{T}}^{\mathrm{miss}}$ cuts, the multijet background is found to be negligible. To maximise the sensitivity further selection criteria depends on the jet multiplicity. Slightly different requirements are used for $m_H < 200\,\mathrm{GeV}$, $200\,\mathrm{GeV} \leq m_H \leq 300\,\mathrm{GeV}$, and $300\,\mathrm{GeV} < m_H < 600\,\mathrm{GeV}$; in the following only the requirements for the low mass region are described.

Due to spin correlations in the $WW^{(\star)}$ system arising from the spin-0 nature of the Higgs boson, the charged leptons tend to emerge from the interaction point in the same direction. This kinematic feature is exploited by requiring that the azimuthal angular difference between the leptons, $\Delta\phi_{\ell\ell}$, be less than 1.8 radians, and that the dilepton invariant mass, $m_{\ell\ell}$, be less than 50 GeV for the 0-jet and 1-jet channels. For the 2-jet channel (wich includes also higher jet multiplicities), the $m_{\ell\ell}$ upper bound is increased to 80 GeV. In the 0-jet channel, the magnitude $p_{\mathrm{T}}^{\ell\ell}$ of the transverse momentum of the dilepton system is required to be greater than 30 GeV for the $e\mu$ channel and greater than 45 GeV for the ee and $\mu\mu$ channels. This improves the rejection of the Drell-Yan background. In the 1-jet channel, backgrounds from top quark decays are suppressed by rejecting events containing a b-tagged jet [4]. The total transverse momentum is required to be smaller than 30 GeV to suppress $t\bar{t}$, single top, and Drell-Yan background events with jets with p_{T} below threshold. A $Z \to \tau\tau$ invariant mass veto is also applied. The 2-jet selection follows the 1-jet selection described above; in addition, a central jet veto selection is applied.

A transverse mass variable m_{T} [5] is used in this analysis to test for the presence of a signal. Figure 1 shows the distributions of the transverse mass after all the low m_H selection criteria in the 0-jet and 1-jet analyses, for all lepton flavours combined.

For the 0-jet and 1-jet analyses, all the main backgrounds from SM processes producing two isolated high-p_{T} leptons (WW, top, Drell-Yan) are estimated using partially data-driven techniques based on normalising the MC predictions to the data in control regions dominated by the relevant background source. Only the small background from

TABLE I. – *Main relative systematic uncertainties on the predicted numbers of signal* (m_H = 125 GeV) *and background (Bkg.) events for each of the three jet multiplicity analyses.*

	Source	Signal (%)	Bkg. (%)
0-jet	Inclusive ggF signal ren./fact. scale	19	0
	1-jet incl. ggF signal ren./fact. scale	10	0
	W+jets fake factor	0	10
	Parton distribution functions	8	2
	WW normalisation	0	6
	Jet energy scale	6	0
1-jet	1-jet incl. ggF signal ren./fact. scale	27	0
	2-jet incl. ggF signal ren./fact. scale	15	0
	Pile-up	5	2
	Missing transverse momentum	8	3
	W+jets fake factor	0	7
	b-tagging efficiency	0	7
	Parton distribution functions	7	1
2-jet	Jet energy scale	13	36
	Pile-up	5	0
	$Z/\gamma^{\star}$+2 jets MC modelling	0	24
	Diboson ren./fact. scale	0	22

diboson processes other than WW is estimated using MC simulation. For the 2-jet analysis, the WW and Drell-Yan backgrounds are also estimated using MC simulation. The backgrounds from fake leptons, which include true leptons from heavy flavour decays in jets, are fully estimated from data. The control samples are obtained from the data with selections similar to those used in the signal region but with some criteria reversed or modified to obtain signal-depleted, background-enriched samples.

3. – Results and conclusions

The main theoretical and experimental systematic uncertainties are shown in table I. Theoretical uncertainties on the signal production cross sections are determined following refs. [6, 7] and include QCD renormalisation and factorisation (ren./fact.) scales variations and the uncertainties on the cross sections in exclusive jet multiplicity. PDF uncertainties are estimated, following refs. [8-11], by the envelopes of error sets as well as different PDF sets. The main experimental uncertainties are related to the jet energy scale. The reconstruction, identification, trigger efficiencies and momentum scales for leptons are estimated to be small (1%). Jet energy scale and lepton momentum scale uncertainties are propagated to the $E_{\mathrm{T}}^{\mathrm{miss}}$ computation which take into account also additional contributions arising from soft terms and pile-up contributions. The efficiency of the b-tagging algorithm is calibrated using samples containing muons reconstructed in the vicinity of jets [12]. Finally, the uncertainty on the integrated luminosity is 3.9% [13, 14].

A fit to the m_{T} distribution is performed in order to obtain the signal yield for each mass hypothesis. The uncertainty on the shape of the total background is dominated by the uncertainties on the normalisations of the individual backgrounds.

The expected numbers of signal (m_H = 125 GeV) and background events and the observed data, after all the requirements of the low m_H selection, are presented in table II.

The statistical analysis of the data employs a binned likelihood function constructed as the product of Poisson probability terms in each lepton flavour channel.

TABLE II. – *The expected numbers of signal and background events after all the requirements of the low m_H selection, as well as the observed (Obs.) numbers of events. The signal is for $m_H = 125\,\mathrm{GeV}$. Only statistical uncertainties associated with the number of events in the MC samples and in the data control regions are shown.*

	Signal	WW	$WZ/ZZ/W\gamma$	$t\bar{t}$	$tW/tb/tqb$	$Z/\gamma^\star$ + jets	W + jets	Total Bkg.	Obs.
0-jet	39.0 ± 0.2	276 ± 17	33 ± 2	27 ± 2	18 ± 2	28 ± 6	44 ± 1	425 ± 26	429
1-jet	10.1 ± 0.1	44 ± 7	13 ± 2	31 ± 2	17 ± 1	10 ± 2	10 ± 1	126 ± 10	145
≥ 2 jets	0.8 ± 0.1	0.8 ± 0.1	0.1 ± 0.1	0.9 ± 0.2	0.1 ± 0.1	negl.	negl.	1.8 ± 0.3	1

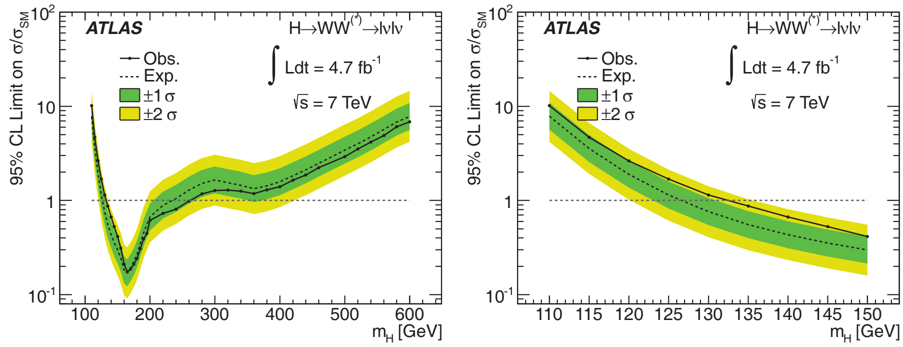

Fig. 2. – Observed (solid) and expected (dashed) 95% CL upper limits on the Higgs boson production cross section, normalised to the SM cross section, as a function of m_H, over the full mass range considered in this analysis (right) and restricted to the range $m_H < 150\,\mathrm{GeV}$ (left). The inner (dark) and outer (light) regions indicate the $\pm 1\sigma$ and $\pm 2\sigma$ uncertainty bands on the expected limit, respectively.

No significant excess of events over the expected background is observed over the entire mass range. Figure 2 shows the observed and expected cross section upper limits at 95% CL, as a function of m_H and normalised to the SM cross section, for the combined 0-jet, 1-jet and 2-jet analyses. The limits exclude a Standard Model Higgs boson with a mass in the range from 133 GeV to 261 GeV at 95% CL, while the expected exclusion range in the absence of a signal is $127\,\mathrm{GeV} \leq m_H \leq 233\,\mathrm{GeV}$.

REFERENCES

[1] Englert F. and Brout R., *Phys. Rev. Lett.*, **13** (1964) 312.
[2] Higgs P. W., *Phys. Rev. Lett.*, **13** (1964) 508.
[3] ATLAS Collaboration, arXiv:1206.0756v1 [hep-ex], submitted to *Phys. Lett. B*.
[4] ATLAS Collaboration, ATLAS-CONF-2011-102.
[5] Barr A. J., Gripaios B. and Lester C. G., *JHEP*, **07** (2009) 072.
[6] LHC Higgs Cross Section Working Group: Dittmaier S., Mariotti C., Passarino G. and Tanaka R. (Editors), arXiv:1101.0593 [hep-ph].
[7] LHC Higgs Cross Section Working Group: Dittmaier S., Mariotti C., Passarino G. and Tanaka R. (Editors), arXiv:1201.3084 [hep-ph].
[8] Botje M. *et al.*, arXiv:1101.0538 [hep-ph].
[9] Lai H. L. *et al.*, arXiv:1007.2241 [hep-ph].
[10] Martin A. D. *et al.*, *Eur. Phys. J. C*, **63** (2009) 189.
[11] Ball R. D. *et al.*, *Nucl. Phys. B*, **849** (2011) 296.
[12] ATLAS Collaboration, ATLAS-CONF-2012-043.
[13] ATLAS Collaboration, *Eur. Phys. J. C*, **71** (2011) 1630.
[14] ATLAS Collaboration, ATLAS-CONF-2011-116.